

Numerical Calculation of Turbulent Flows in Compound Channels with an Algebraic Stress Turbulence Model

Yoshihisa KAWAHARA, Assistant Professor
and
Nobuyuki TAMAI, Professor

Department of Civil Engineering, University of Tokyo
7-3-1 Hongo, Bunkyo-ku, Tokyo, 113, Japan

ABSTRACT

A numerical model is presented for calculating flows in compound prismatic channels with turbulence-driven secondary motion. The model uses the algebraic stress turbulence model developed by Launder and Ying and the $k-\varepsilon$ model along with the continuity and momentum equations. The model is tested by application to an open channel flow and a duct flow. Satisfactory predictions are obtained on the distributions of mean velocities and shear stresses opposing the primary velocity, while the anisotropy of normal stresses is underestimated by one order of magnitude less than the experimental data.

1. Introduction

Many rivers in Japan have been improved to have a compound cross-section which consists of a deep main channel and shallow flood plains. River flow is contained within the main channel in low flow regime. During the flood events, however, the flow spills over onto the flood plains, resulting in a compound channel flow. Such a flow is accompanied by secondary currents and has highly three-dimensional structure. Further, the flow changes its structure with the variation of the channel configuration, the roughness distribution, etc. These complexities of the flow field have been an obstacle to clarify the full features of the flow. Hence a numerical model has to be developed which can predict important characteristics of the flow under a wide range of hydraulic conditions.

The purpose of the present paper is to demonstrate that main characteristics of the mean velocity fields in compound straight channels can be reproduced with the ASM developed by Launder and Ying³⁾. Calculated results are compared with two available experimental data, one for an open channel and the other for a closed channel, with the emphasis on the distributions of mean velocities and turbulent stresses to examine the applicability of the stress model.

2. Model Description

2.1 Governing Equations

The compound channel cross-section and the coordinate system are shown in Fig.1. The cross-sectional shape is symmetrical.

The present numerical model solves the continuity equation, three momentum equations and transport equations for the kinetic energy of turbulence k and the dissipation rate ε . All these equations can be written in a general form as shown below.

$$\frac{\partial}{\partial x}(U\phi) + \frac{\partial}{\partial y}(V\phi - \Gamma \frac{\partial \phi}{\partial y}) + \frac{\partial}{\partial z}(W\phi - \Gamma \frac{\partial \phi}{\partial z}) = s(\phi), \quad (1)$$

where U , V , W are mean velocities in the x , y and z directions, respectively; ϕ is a variable; Γ is a diffusion coefficient and s is a source term.

The quantities ϕ , Γ and s are specific to each governing equation and are expressed as follows:

$$\phi=1, \quad \Gamma=0, \quad s=0 \quad (2)$$

$$\phi=U, \quad \Gamma=\nu+\nu_t, \quad s=g\sin\theta - g\cos\theta \frac{\partial D_c}{\partial x} \quad (3)$$

$$\phi=V, \quad \Gamma=\nu, \quad s=-\frac{1}{\rho} \frac{\partial P}{\partial y} + \frac{\partial}{\partial y}(-\overline{v^2}) + \frac{\partial}{\partial z}(-\overline{vw}) \quad (4)$$

$$\phi=W, \quad \Gamma=\nu, \quad s=-\frac{1}{\rho} \frac{\partial P}{\partial z} + \frac{\partial}{\partial y}(-\overline{vw}) + \frac{\partial}{\partial z}(-\overline{w^2}) \quad (5)$$

$$\phi=k, \quad \Gamma=\nu+\nu_t/\sigma_k, \quad s=G - \varepsilon \quad (6)$$

$$\phi=\varepsilon, \quad \Gamma=\nu+\nu_t/\sigma_\varepsilon, \quad s=(c_{\varepsilon 1}G - c_{\varepsilon 2}\varepsilon) \varepsilon/k, \quad (7)$$

where u , v and w are fluctuating components of velocity; P is the pressure; g is the gravitational acceleration; D_c is the flow depth in the main channel; θ is the inclination of the channel bed to a horizontal line; ν is the kinematic viscosity of the fluid; ν_t is the eddy viscosity; G is the

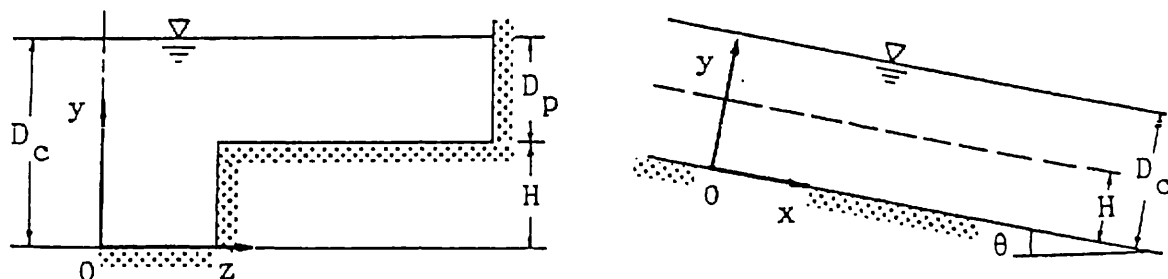


Fig.1 The coordinate system.

production rate of turbulence energy and σ_k , σ_ε , $c_{\varepsilon 1}$, $c_{\varepsilon 2}$ are empirical constants. The eddy viscosity and the production rate of turbulence energy are evaluated as

$$\nu_t = c_\mu \frac{k^2}{\varepsilon}, \quad G = \nu_t \left[\left(\frac{\partial U}{\partial y} \right)^2 + \left(\frac{\partial U}{\partial z} \right)^2 \right], \quad (8,9)$$

where c_μ is an empirical constant.

In deriving the above equations, the flow is assumed predominant in the x-direction and hence the x-gradient stress terms are neglected. It is further assumed that the pressure gradient term in the x-component of momentum equation is represented by the term $g \sin \theta - g \cos \theta \frac{dDc}{dx}$. The x-component of momentum equation is applicable also for a closed channel flow when the pressure gradient term is replaced by $-1/\rho d\phi/dx$, where ϕ is the cross-sectional mean pressure.

Before the equations are solved, a turbulence model must be introduced for determining the Reynolds stresses. We adopt the ASM developed by Launder and Ying for its simplicity and easy applicability. The Reynolds stresses are expressed by the following relations.

$$\begin{aligned} -\overline{u^2} &= -c_{k0}' k, & -\overline{uv} &= \nu_t \frac{\partial U}{\partial y}, & -\overline{uw} &= \nu_t \frac{\partial U}{\partial z}, \\ -\overline{v^2} &= c' \nu_t \frac{k}{\varepsilon} \left(\frac{\partial U}{\partial y} \right)^2 - c_k' k, & -\overline{vw} &= c' \nu_t \frac{k}{\varepsilon} \left(\frac{\partial U}{\partial y} \right) \left(\frac{\partial U}{\partial z} \right), & (10) \\ -\overline{w^2} &= c' \nu_t \frac{k}{\varepsilon} \left(\frac{\partial U}{\partial z} \right)^2 - c_k' k, \end{aligned}$$

where c_{k0}' , c_k' and c' are empirical constants. It is the distinctive feature of Launder-Ying model that the constant c' governs the intensity of the secondary current.

The values for the empirical constants are given as follows:

$$\begin{aligned} c_\mu &= 0.09, & c_{\varepsilon 1} &= 1.45, & c_{\varepsilon 2} &= 1.9, & \sigma_k &= 1.4, & \sigma_\varepsilon &= 1.3 \\ c_{k0}' &= 0.915, & c_k' &= 0.522, & c' &= 0.037. \end{aligned} \quad (11)$$

2.2 Boundary Conditions

Boundary conditions must be specified for the mean velocity components, the turbulence energy and the dissipation rate at inlet, solid walls, planes of symmetry and free surface for an open channel flow. At inlet, uniform distribution is given for all quantities. At planes of symmetry, the velocity component normal to the symmetry plane is zero, while for all other quantities, the gradient normal to the plane is taken as zero.

At solid walls, the wall-function technique is adopted which relates the streamwise velocity U , the kinetic energy

k and the dissipation rate ε at the first grid point to the local friction velocity U^* by

$$\frac{U}{U^*} = \frac{1}{\kappa} \ln(Ey^{\dagger}), \quad k = \frac{U^{*2}}{\sqrt{c_{\mu}}}, \quad \varepsilon = \frac{U^{*3}}{\kappa y}, \quad y^{\dagger} = \frac{U^* y}{\nu}, \quad (12)$$

where κ is the von Karman constant (here 0.42); E is a friction parameter (here 9.0 for smooth walls), y is the distance from the wall. No-slip conditions is applied on solid walls for the other mean velocity components.

At free surface of an open channel flow, symmetry conditions are applied for all variables except for the dissipation rate. Following Naot and Rodi⁵⁾, the dissipation rate is specified as

$$\varepsilon = \frac{c_{\mu}^{3/4} k^{3/2}}{\kappa} \left(\frac{1}{y'} + \frac{1}{0.07D} \right), \quad (13)$$

in which D is the flow depth and y' is the distance from the bank.

2.3 Calculation Procedure

Calculations are carried out on the non-uniform and staggered grid. Discretized equation is obtained by integrating Eq.1 over the small grid volume.

The Spalding-Patankar algorithm for three-dimensional parabolic flow⁶⁾ is applied to solve the equations simultaneously. Convection-diffusion terms in Eq.1 are evaluated by the power-law scheme proposed by Patankar⁷⁾.

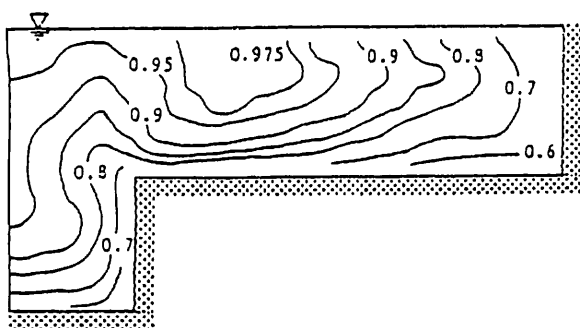
Calculation marches forward to a distance of about 400-500 times the hydraulic radius, where mean velocities are fully developed. Calculated results at the downstream end are compared with those of the experiment.

3. Application of the Model

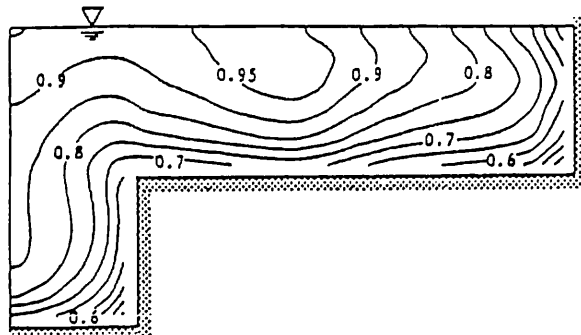
3.1 Compound Open Channel Flow

Tominaga et al.⁸⁾ made detailed measurements of the distributions of mean velocities and turbulent stresses for open channel flows. We first applied the numerical model to one of their experiments. The channel had the flood plain of 5.01cm high, main channel of 8.7cm wide and flood plain of 10.8cm wide. The total depth was 10.03cm and the mean velocity was 34.35cm/s, thus the Reynolds number based on the hydraulic radius and the mean velocity was 5.09×10^4 .

Fig.2 compares the isovels U/U_{\max} (U_{\max} is the maximum velocity) with the measured results. The comparison shows good agreement, even though the maximum velocity is somewhat overestimated, and consequently the velocity level is underpredicted over the whole domain. Also, the distor-

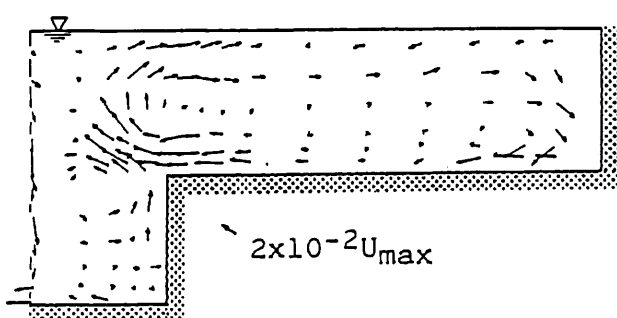


(a) Experiment

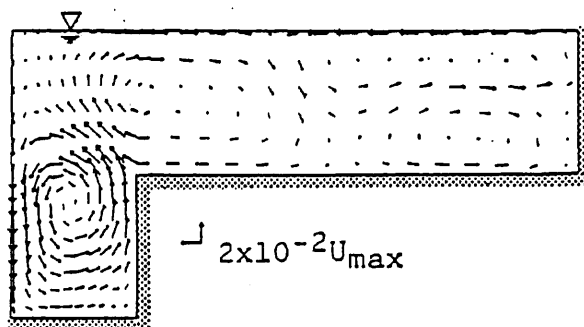


(b) Calculation

Fig.2 Primary velocity U/U_{max} .

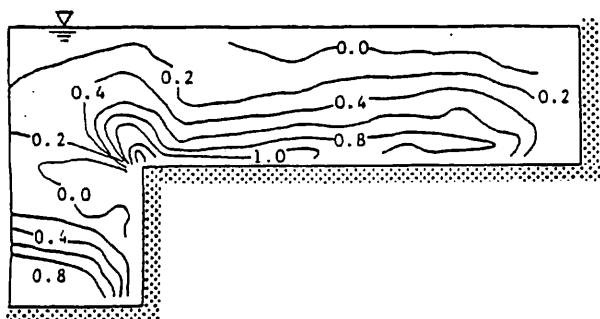


(a) Experiment

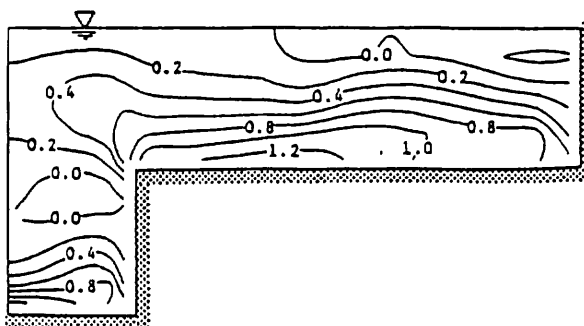


(b) Calculation

Fig.3 Secondary flow.

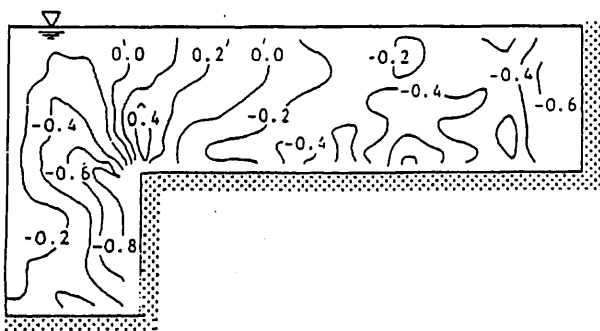


(a) Experiment

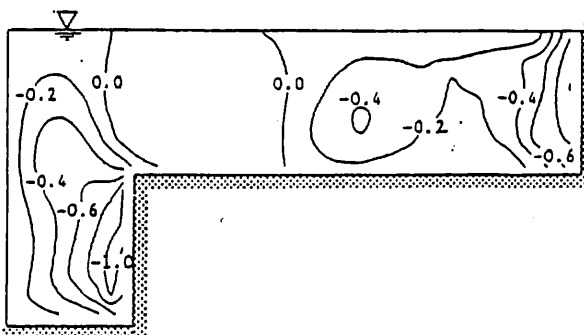


(b) Calculation

Fig.4 Shear stress $-\overline{uv}/U_f^2$.



(a) Experiment



(b) Calculation

Fig.5 Shear stress $-\overline{uw}/U_f^2$.

tion of the contours near the interface between the main channel and the flood plain and the bulging toward the main channel corner are predicted to a lower degree.

Fig.3 displays the secondary flow vectors, where the reference velocity is taken as the $0.02U_{max}$. The predicted secondary flow cells agree well with the experiment. The magnitude of the secondary flow is underestimated at the interface, while it is overestimated near the symmetry axis of the main channel. The differences are consistent with the discrepancies in the isovels of the primary flow.

The distributions of the shear stress $-\overline{uv}/U_f^2$ (U_f is the mean friction velocity) are shown in fig.4. The prediction yields the correct change of sign in the shear field and the predicted contours shows good agreement with the measurement. Fig.5 compares the contours of the shear stress $-\overline{uw}/U_f^2$. The prediction compares favorably with the experiment in the main channel. In the flood plain, the correct sign change is simulated, while the predicted level of the stress is lower near the interface and the complex distribution in the middle part is not well reproduced.

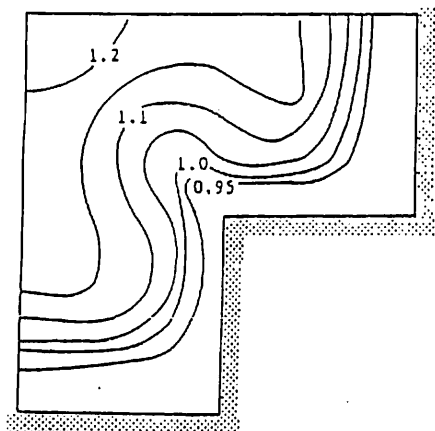
3.2 Compound Closed Channel Flow

Nakayama et al.⁴⁾ investigated the flow in a closed channel of a cross-shaped cross-section. The duct had the main channel and the flood plain of the same 1.8cm wide. The Reynolds number based on the hydraulic diameter and the mean velocity was 3.0×10^4 .

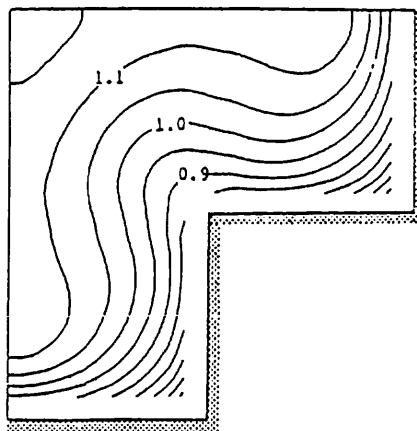
Fig.6 shows the contours of the primary velocity U/U_m (U_m is the cross-sectional mean velocity) with the experiment. The prediction compares well with the measurement, despite the fact that the predicted level of the isovels is lower than that of the experiment and that their distortions toward the main channel center and the corners are slightly underestimated.

Secondary flow vectors are compared in Fig.7. A pair of secondary flow cells is well predicted. The up-welling motion at the end of the flood plain, which is also noticeable in Fig.3, is inherent to compound channel flows. The magnitude of the secondary current along the symmetry axes is overpredicted, which produces the steep gradient of the primary flow near the walls.

Fig.8 shows the anisotropy of normal stress components $(v^2 - w^2)/U_m^2$, the gradient of which is the major cause of the secondary flow. A careful comparison reveals that the predicted level of contours is about one order less than that of the experiment, the discrepancy which seems to be inherent of this particular ASM. As indicated by Launder²⁾ and Demueren-Rodi¹⁾, the ASM is designed and tuned on the basis of simple yet accurate prediction on mean flow fields

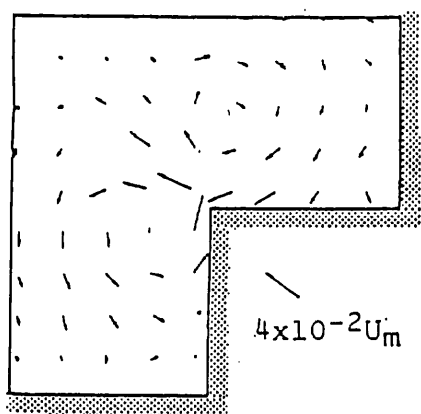


(a) Experiment

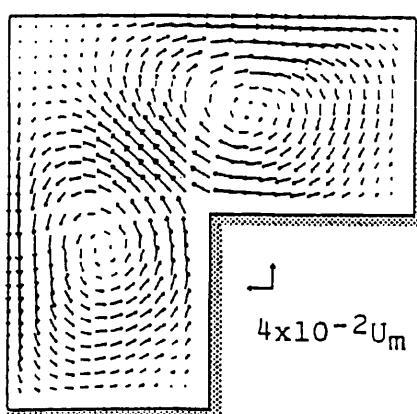


(b) Calculation

Fig.6
Primary
velocity
 U/U_m .

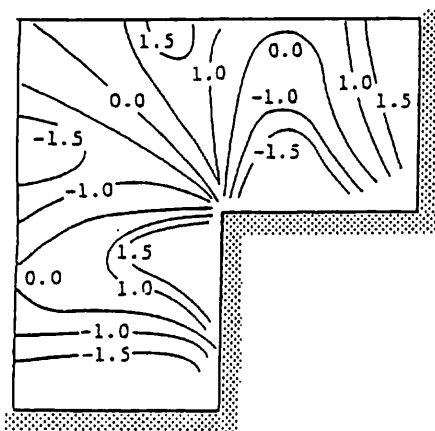


(a) Experiment

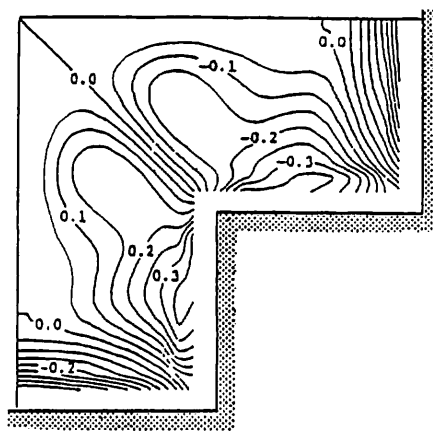


(b) Calculation

Fig.7
Secondary
flow.

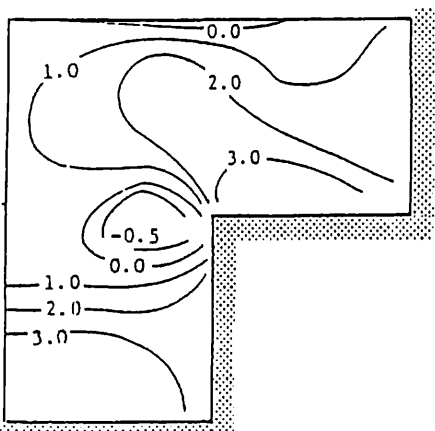


(a) Experiment

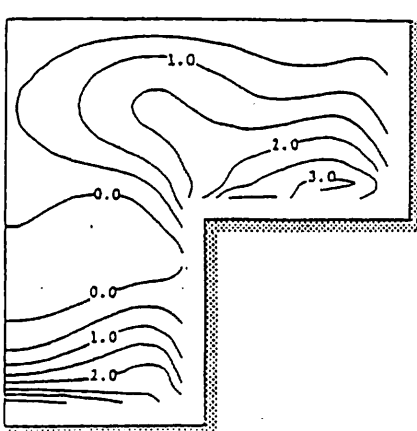


(b) Calculation

Fig.8
Anisotropy
of normal
stresses
 $[(\overline{v^2} - \overline{w^2})/U_m^2]$
 $\times 10^3$.



(a) Experiment



(b) Calculation

Fig.9
Shear stress
 $-\overline{uv}/U_m^2$.

at the expense of the loss of accuracy in some of the turbulence structures.

Fig.9 compares the shear stress $-\overline{uv}/U_m^2$. The prediction is in good agreement with the experiment, even though the level of the contours in the lower part of the main channel is overpredicted, where the high shear rate of the primary flow is calculated because of the overestimation of the secondary current.

4. Concluding Remarks

A numerical model has been presented for simulating turbulent flows in compound straight channels and tested by application to a developed open channel flow and also to a developed duct flow. The comparisons with the measurements have revealed that the present model is able to predict the mean velocity fields in compound channel flows, while this model cannot explain correctly the generation mechanism of turbulence-driven secondary flow in compound channels. Further refinements of the numerical model are thus required to investigate the turbulence structures in compound channels.

References

1. Demueren, A.O. and Rodi, W. (1984), "Calculation of Turbulence-Driven Secondary Motion in Non-Circular Ducts", Journal of Fluid Mechanics, Vol.140, pp.189-222.
2. Launder, B. E. (1976), Discussion on Gessner and Emery's work(1976), Transactions of Amer. Soc. Mechanical Engineers, Journal of Fluids Engineering, Vol.98, pp.276-277.
3. Launder, B.E. and Ying, W.M. (1973), "Prediction of FLOW and Heat Transfer in Ducts of Square-Section", Proc. Institution of Mechanical Engineers, Vol.187, pp.455-461.
4. Nakayama, A., Kojima, H. and Watanabe, T. (1987), "Fluid Flow and Heat Transfer within Ducts of a Cross-Shaped Cross-Section", Transactions of Jpn. Soc. Mechanical Engineers, Vol.53B, No.489, pp.1573-1579 (in Japanese).
5. Naot, D. and Rodi, W. (1982), "Calculation of Secondary Currents in Channel Flow", Journal of Hydraulics Div., Amer. Soc. Civil Engineers, Vol.108, No.8, pp.948-968.
6. Patankar, S.V. and Spalding, B.D. (1972), "A Calculation Procedure for Heat, Mass and Momentum Transfer in Three-Dimensional Parabolic Flows", International Journal of Heat and Mass Transfer, Vol.15, pp.1787-1806.
7. Patankar, S.V. (1980), Numerical Heat Transfer and Fluid Flow, Hemisphere, Washington D.C.
8. Tominaga, A., Ezaki, K. and Nakamura, E. (1987), "Three-Dimensional Turbulent Structures in Compound Open Channel Flows", Proc. 42nd Annual Conf., Jpn. Soc. Civil Engineers, II, pp.372-373(in Japanese).